the FEBS Journal

An E3 ubiquitin ligase, Synoviolin, is involved in the degradation of immature nicastrin, and regulates the production of amyloid β-protein

Tomoji Maeda[1], Toshihiro Marutani[2,*], Kun Zou[1], Wataru Araki[3], Chiaki Tanabe[1], Naoko Yagishita[4], Yoshihisa Yamano[4], Tetsuya Amano[4], Makoto Michikawa[2], Toshihiro Nakajima[4,5,6] and Hiroto Komano[1]

1 Department of Neuroscience, School of Pharmacy, Iwate Medical University, Morioka, Japan
2 Department of Alzheimer's Disease Research, National Center for Geriatrics and Gerontology, Aichi, Japan
3 Department of Demyelinating Disease and Aging, National Institute of Neuroscience, Tokyo, Japan
4 Institute of Medical Science, St. Marianna University School of Medicine, Kawasaki, Japan
5 Choju Medical Institute and Fukushimura Hospital, Toyohashi, Japan
6 Misato Marine Hospital, Kochi, Japan

Keywords
amyloid β-protein; E3 ubiquitin ligase; nicastrin; presenilin; γ-secretase

Correspondence
H. Komano, Department of Neuroscience, School of Pharmacy, Iwate Medical University, 2-1-1 Nishitokuta, Yahaba, Shiwa, Iwate 028-3694, Japan
Fax: +81 19 698 1864
Tel: +81 19 651 5111, extn 5210
E-mail: hkomano@iwate-med.ac.jp

***Present address**
Department of Biology, Faculty of Sciences, Kyushu University Graduate School, Fukuoka, Japan

(Received 13 January 2009, revised 2 August 2009, accepted 6 August 2009)

doi:10.1111/j.1742-4658.2009.07264.x

The presenilin complex, consisting of presenilin, nicastrin, anterior pharynx defective-1 and presenilin enhancer-2, constitutes γ-secretase, which is required for the generation of amyloid β-protein. In this article, we show that Synoviolin (also called Hrd1), which is an E3 ubiquitin ligase implicated in endoplasmic reticulum-associated degradation, is involved in the degradation of endogenous immature nicastrin, and affects amyloid β-protein generation. It was found that the level of immature nicastrin was dramatically increased in *synoviolin*-null cells as a result of the inhibition of degradation, but the accumulation of endogenous presenilin, anterior pharynx defective-1 and presenilin enhancer-2 was not changed. This was abolished by the transfection of exogenous Synoviolin. Moreover, nicastrin was co-immunoprecipitated with Synoviolin, strongly suggesting that nicastrin is the substrate of Synoviolin. Interestingly, amyloid β-protein generation was increased by the overexpression of Synoviolin, although the nicastrin level was decreased. Thus, Synoviolin-mediated ubiquitination is involved in the degradation of immature nicastrin, and probably regulates amyloid β-protein generation.

Structured digital abstract

- MINT-7255352: *Synoviolin* (uniprotkb:Q9DBY1) *physically interacts* (MI:0915) with *NCT* (uniprotkb:P57716) by *anti tag coimmunoprecipitation* (MI:0007)
- MINT-7255377: *Ubiquitin* (uniprotkb:P62991) *physically interacts* (MI:0915) with *NCT* (uniprotkb:P57716) by *anti bait coimmunoprecipitation* (MI:0006)
- MINT-7255363: *NCT* (uniprotkb:P57716) *physically interacts* (MI:0915) with *Synoviolin* (uniprotkb:Q9DBY1) by *anti bait coimmunoprecipitation* (MI:0006)

Introduction

Amyloid β-protein (Aβ), which is the major component of senile plaques in the brains of patients with Alzheimer's disease, is generated from the amyloid precursor protein (APP) through its sequential proteolytic

Abbreviations
Aβ, amyloid β-protein; APH-1, anterior pharynx defective-1; APP, β-amyloid precursor protein; CTF, C-terminal fragment; ER, endoplasmic reticulum; NCT, nicastrin; NTF, N-terminal fragment; PEN-2, presenilin enhancer-2; PS, presenilin.

cleavage catalyzed by β- and γ-secretases [1]. β-Secretase has been identified as a membrane-tethered aspartyl protease [2]. γ-Secretase activity is attributed to the presenilin (PS) complex, which is composed of four transmembrane proteins: PS, nicastrin (NCT), presenilin enhancer-2 (PEN-2) and anterior pharynx defective-1 (APH-1) (collectively named PS cofactors in this study) (reviewed in [3]). Full-length PS is endoproteolytically processed into two fragments: the N-terminal fragment (NTF) and the C-terminal fragment (CTF) [4]. The processed PS resides in the γ-secretase complex (reviewed in [3]). Endogenous PS, NCT, PEN-2 and APH-1 are mainly localized in the endoplasmic reticulum (ER) and Golgi [5], and the properly assembled complex is transported through the secretory pathway to localize predominantly in the Golgi and then at the cell surface [6,7].

NCT is a type I transmembrane protein that possesses many potential glycosylation sites within its large ectodomain [8]. Several studies have established that three principal forms of NCT exist in cells: the unglycosylated, nascent protein (~ 80 kDa); an immature N-linked glycosylated species (immature NCT, ~ 110 kDa); and a mature N-linked isoform (mature NCT, ~ 150 kDa) which is formed after entering the Golgi apparatus [9]. The mature NCT associates with active γ-secretase [10] and, importantly, PS is required for the full post-translational generation of this mature NCT species [9]. In addition, NCT is critical for the stability and trafficking of other γ-secretase components, and NCT affects Aβ production [11].

Interestingly, the cellular level of PS is tightly limited [12]. Excess PS cofactors which fail to reside in the complex, such as full-length PS, mostly undergo ubiquitin/proteasome-mediated degradation, although the precise mechanism of elimination of excess cofactors is not fully understood [12].

Ubiquitination is required for proteasome-mediated degradation, although, recently, accumulating evidence has shown that ubiquitin has multiple functions, including intracellular trafficking (reviewed in [13]), which is accomplished through the sequential actions of enzymes: an activating enzyme (E1), a conjugating enzyme (E2) and a ligase (E3) (reviewed in [14]). Of the three enzymes, E3 enzymes are the key determining factors in substrate protein selection. Synoviolin, a representative of ER-resident E3 ubiquitin ligase, is a mammalian homolog of yeast Hrd1 [15]. Synoviolin is also a pathogenic factor in rheumatoid arthritis [16], and is involved in ER-associated degradation [17]. The substrates of Synoviolin were found to include polyglutamine-expanded huntingtin [18], the tumor suppressor gene p53 [19] and Parkin-associated endothelin receptor-like receptor [20].

In this study, we addressed whether Synoviolin is involved in the degradation of PS cofactors using *synoviolin*-null cells, as PS cofactors undergo the ubiquitin/proteasome pathway. We report that Synoviolin is involved in the degradation of immature NCT and regulates Aβ generation.

Results

Accumulation of immature NCT in *synoviolin*-null cells

To investigate whether Synoviolin is involved in the degradation of PS cofactors, we first compared the levels of PS cofactors by immunoblotting between *synoviolin*-null cells and wild-type (wt) cells. As shown in Fig. 1, the level of endogenous immature NCT was found to be markedly increased in *synoviolin*-null cells, compared with wt cells, although endogenous PS, APH-1 and PEN-2 were not changed in *synoviolin*-null cells. Interestingly, the mobilities of immature and mature NCT on the gel in *synoviolin*-null cells were slightly faster than that in wt cells (Fig. 1A). This is probably a result of the difference in the degree of sugar modification, because deglycosylation treatment of NCT in *synoviolin*-null cells resulted in a similar mobility to that in wt cells (Fig. S1, see Supporting Information). We also determined the levels of γ-secretase-unrelated ER protein (calnexin) and cytoskeleton protein (tubulin) in these cells as the internal control proteins. The calnexin and tubulin levels were found to be similar between these cells, confirming that the same amount of protein was loaded in each lane (Fig. 1A). In addition, the observed accumulation of endogenous immature NCT in *synoviolin*-null cells was abolished by exogenously expressed Synoviolin, but not by the expression of Synoviolin C307A mutant lacking E3 ubiquitin ligase activity [21], indicating that the lack of E3 ubiquitin ligase activity of Synoviolin causes the accumulation of immature NCT (Fig. 1B, right panel). As shown in Fig. 1B (left panel), the overexpression of Synoviolin in wt cells decreased both immature and mature NCT levels; however, very interestingly, the expression of Synoviolin C307A mutant in wt cells caused the accumulation of much more immature NCT than mature NCT. Because the C307A mutant inhibits the ubiquitination mediated by endogenous Synoviolin in a dominant-negative manner, as reported previously [21], this result strongly suggests that Synoviolin-mediated ubiquitination is involved in the preferential degradation of immature NCT.

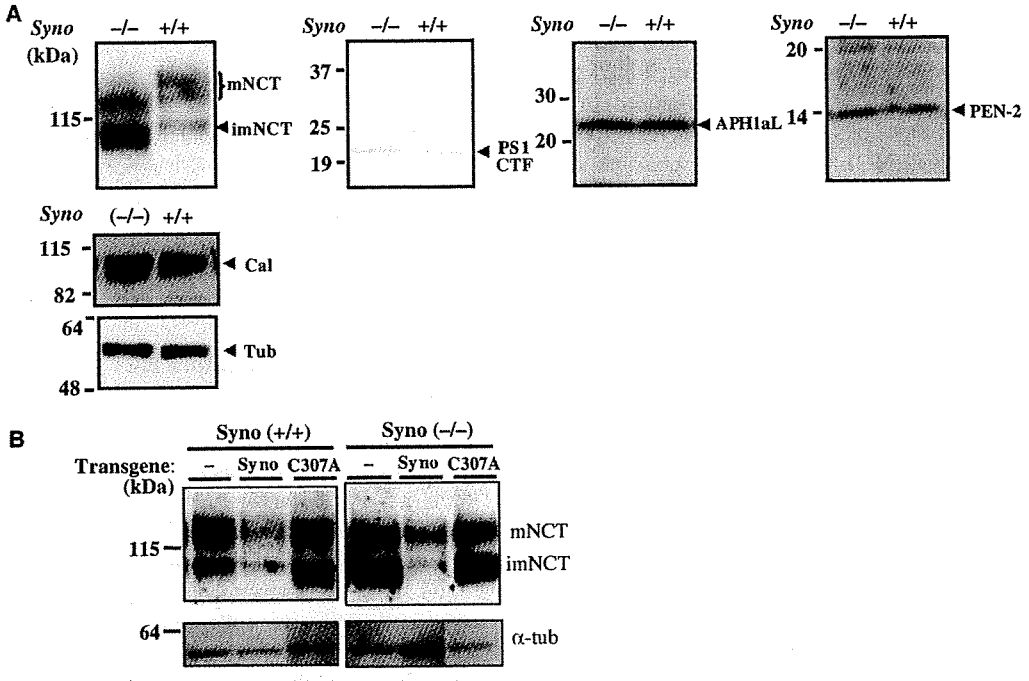

Fig. 1. Accumulation of immature NCT in *synoviolin*-null fibroblasts. (A) The components of the PS complex (NCT, PS-1, APH-1, PEN-2) in the lysate (20 μg) of *synoviolin*-null fibroblasts were detected by immunoblotting with anti-NCT IgG, anti-APH1aL IgG and anti-PEN-2 IgG. Calnexin and α-tubulin in the lysate were also immunodetected as internal markers. −/−, *synoviolin*-null fibroblasts; +/+, wt fibroblasts. (B) NCT in the lysates from wt fibroblasts (left panel) and *synoviolin*-null fibroblasts (right panel), retrovirally expressing Synoviolin or Synoviolin C307A mutant lacking E3 ubiquitin ligase activity, was detected by immunoblotting with anti-NCT IgG. Mutation of the conserved cysteine 307 to alanine in Synoviolin disrupts its ligase activity and this C307A mutant functions in a dominant-negative manner [21]. α-Tubulin in the lysate was also detected as internal marker. imNCT, immature NCT; mNCT, mature NCT; −, mock transfection; Syno, Synoviolin; C307A, Synoviolin C307A mutant; α-tub, α-tubulin.

Effect of Synoviolin on the stability of NCT

Because Synoviolin is an E3 ubiquitin ligase for proteasome-dependent protein degradation, it is most likely that the accumulation of NCT in *synoviolin*-null cells is a result of the suppression of the degradation of NCT. To further investigate this, we next compared the degradation of NCT with time between *synoviolin*-null cells and wt cells. As shown in Fig. 2, western blot analysis of the intracellular degradation of NCT in *synoviolin*-null cells and wt cells following cycloheximide treatment revealed that immature NCT in *synoviolin*-null cells remained stable, as did mature NCT, although, in wt cells, the immature NCT level was preferentially decreased at 10 h after treatment. As a decrease in the immature NCT level seems to include effects of both its maturation and degradation, we further confirmed the degradation of immature NCT in wt cells with treatment by the proteasome inhibitor MG-132. As shown in Fig. 2C, the treatment of wt cells with MG-132 was found to preferentially increase the level of immature NCT compared with that of mature NCT, strongly suggesting that immature NCT is preferentially degraded by the proteasome. Taken together, Synoviolin is most likely to be involved in the preferential degradation of immature NCT via the ubiquitin/proteasome pathway.

Synoviolin interacts with NCT

E3 ligases for ubiquitination confer specificity to the ubiquitin system by directly interacting with the substrate proteins and helping to transfer ubiquitin to them. Therefore, to determine whether NCT is the substrate of Synoviolin, we determined whether Synoviolin interacts with NCT. As shown in Fig. 3, immature NCT was coimmunoprecipitated with anti-FLAG IgG and, in addition, Synovolin was coimmunoprecipitated with anti-NCT IgG when FLAG-tagged Synoviolin and NCT were coexpressed in *synoviolin*-null cells. These results indicate that Synoviolin interacts

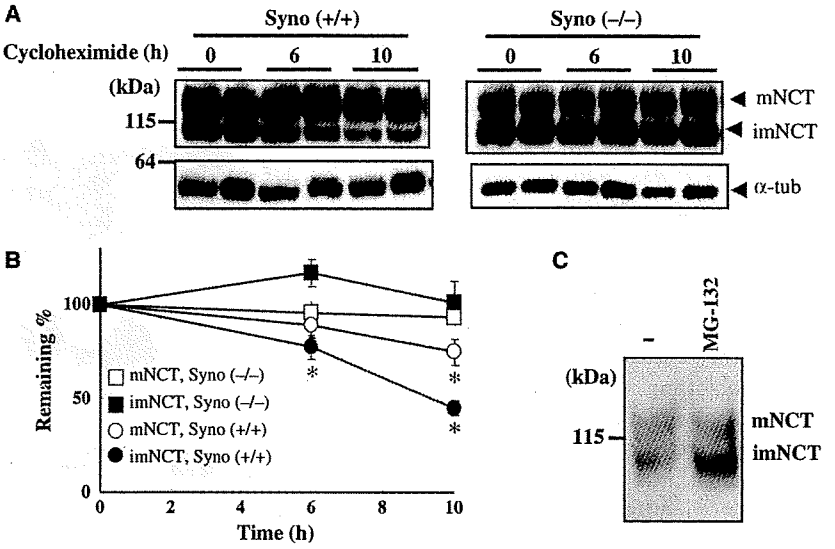

Fig. 2. Degradation of NCT in *synoviolin*-null and wt fibroblasts. (A) *synoviolin*-null and wt fibroblasts were treated with 20 μg·mL^{-1} cycloheximide and harvested at the times indicated. NCT in RIPA-solubilized lysates (10 μg) was detected by immunoblotting with anti-NCT antibody. α-Tubulin in the lysates was also immunodetected as an internal control for a stable protein. Each sample was duplicated. imNCT, immature NCT; mNCT, mature NCT; α-Tub, α-tubulin. (B) The intensities of the bands corresponding to immature NCT and mature NCT in (A) were densitometrically quantified using a luminescent image analyzer LAS-3000 (Fuji Photo Film Co., Ltd., Tokyo, Japan). NCT levels remaining at each time point were calculated as a percentage of the intensity at time zero. Each value is the average of four independent experiments. Asterisk indicates significant differences from time zero [significant difference at $P < 0.05$ (Student's *t*-test)]. (C) Wt fibroblasts were treated with 10 μM MG-132 for 10 h, and NCT in the RIPA-solubilized lysates (10 μg) was detected by immunoblotting with anti-NCT antibody. –, cells treated without MG-132.

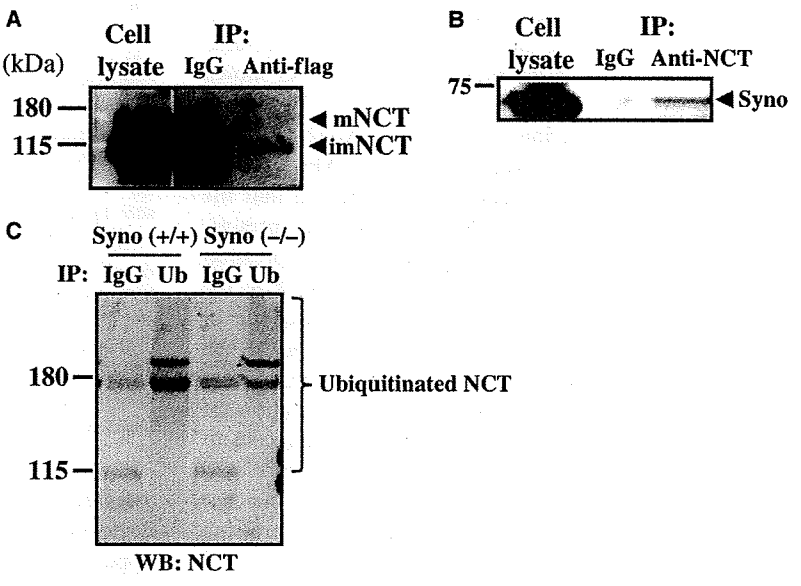

Fig. 3. Synoviolin interacts with NCT. (A) The cell lysates of *synoviolin*-null fibroblasts transiently coexpressing FLAG-tagged Synoviolin and NCT were immunoprecipitated with anti-FLAG antibody and immunodetected with anti-NCT antibody. (B) The same cell lysates were immunoprecipitated with anti-NCT antibody and then immunodetected with anti-Synoviolin antibody. (C) After *synoviolin*-null and wt fibroblasts transiently transfected with NCT had been treated with cycloheximide and lactacystin for 8 h, the cells were harvested. The RIPA-solubilized lysates (1 mg) were immunoprecipitated with anti-ubiquitin mouse antibody (mouse IgG for control) and then immunodetected with anti-NCT antibody. IP, immunoprecipitation; WB, western blot.

with immature NCT. In addition, the degree of ubiquitination of NCT in wt cells was also found to be slightly higher than that in *synoviolin*-null cells (Fig. 3C). However, it was also noted that NCT was slightly ubiquitinated even in *synoviolin*-null cells. Therefore, it is most likely that NCT is a substrate of Synoviolin, but the other E3 ubiquitin ligase also appears to ubiquitinate NCT.

Detection of NCT on the cell surface in *synoviolin*-null cells

Only mature NCT goes to the cell surface, and immature NCT stays within the cells, as reported previously [6,22]. As the level of immature NCT was greatly increased and the molecular weight of NCT was changed slightly in *synoviolin*-null cells, we investigated whether the cellular localization of NCT was different between *synoviolin*-null cells and wt cells. To determine this, we detected NCT localized at the plasma membrane in *synoviolin*-null cells. For this purpose, we labeled the cell surface proteins with biotin, and then detected the surface-biotinylated NCT by immunoblotting with anti-NCT IgG. As shown in Fig. 4A, we found that both immature and mature NCT were clearly detected on the cell surface in *synoviolin*-null cells, although, in wt cells, only mature NCT was detected on the cell surface. In addition, the mature NCT level on the cell surface was increased in *synoviolin*-null cells (Fig. 4B) [percentage of mature NCT at the cell surface relative to that in the total lysate: 24% (wt) versus 64% (Syn−/−)]. These results indicate that a functional deletion of Synoviolin causes a change in the intracellular trafficking of NCT.

Effect of Synoviolin on the production of Aβ

NCT is one of the essential cofactors of the γ-secretase complex. We therefore investigated the effect of the Synoviolin-mediated degradation of NCT on Aβ generation. In Fig. 5, we measured the Aβ level secreted from wt fibroblasts overexpressing APP [23]. As shown in Fig. 5A, B, the overexpression of Synoviolin enhanced the production of Aβ40 and Aβ42 by about twofold, whereas the secretion of soluble APP was not changed in these cells. Figure 5C also showed that the endogenous NCT level was decreased and the intracellular APP level was not changed by the overexpression of Synoviolin. Previously, the targeting of NCT to the cell surface enhanced Aβ generation, because one of the main Aβ generation sites is likely to be in the cell surface [6]. Therefore, it is possible that the overexpression of Synoviolin enhances the localization of NCT at the cell surface, resulting in an enhancement of Aβ generation. To test this possibility, we measured the level of NCT on the cell membrane. No increase in the cell surface NCT level in cells overexpressing Synoviolin was observed (Fig. 5D).

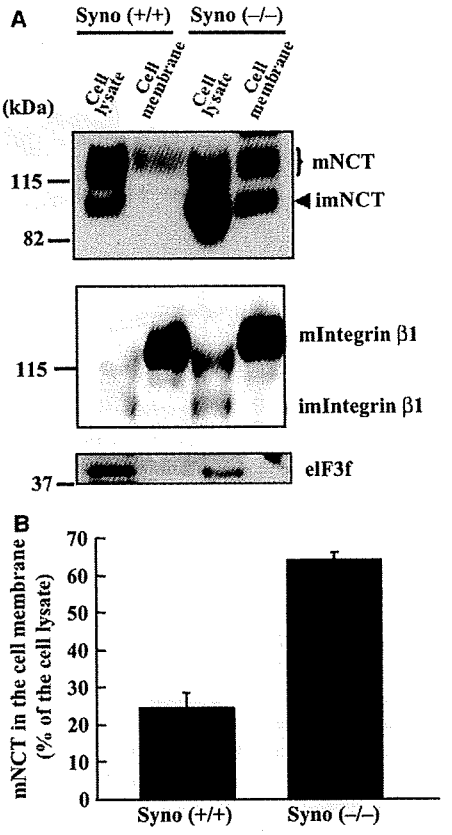

Fig. 4. Cell surface distribution of immature and mature NCT in *synoviolin*-null fibroblasts. (A) Cell surface proteins of *synoviolin*-null and wt fibroblasts were biotinylated as described in Materials and methods. The lysates of surface-biotinylated cells were then incubated with streptavidin–agarose. Total lysate (20 μg) and biotinylated proteins (streptavidin–agarose bound) were immunodetected with anti-NCT IgG, anti-integrin β1 IgG (as a control for the cell surface protein) [22] and anti-eIF3f IgG (as a control for the cytosolic protein) [32]. imNCT, immature NCT; mNCT, mature NCT; m integrin β1, mature integrin β1; im integrin β1, immature integrin β1. (B) Band intensities were densitometrically quantified with a luminescent image analyzer LAS-3000 (Fuji Photo Film Co., Ltd.), and the percentage mature NCT level in the cell membrane relative to that in the total cell lysate was calculated. Data are the average of two independent experiments. The percentage immature NCT level in the cell membrane relative to that in the total cell lysate in *synoviolin*-null cells was 22.0 ± 4.5%.

Discussion

In this study, we showed that Synoviolin is involved in the intracellular degradation of NCT. Of the four γ-secretase components, only NCT was found to be degraded by Synoviolin. In addition, Synoviolin appears to preferentially target immature NCT for degradation, because *synoviolin*-null cells exhibited the accumulation of immature NCT, and the expression of the dominant-negative Synoviolin mutant lacking E3 ubiquitin ligase activity in wt cells caused a greater accumulation of immature NCT than mature NCT.

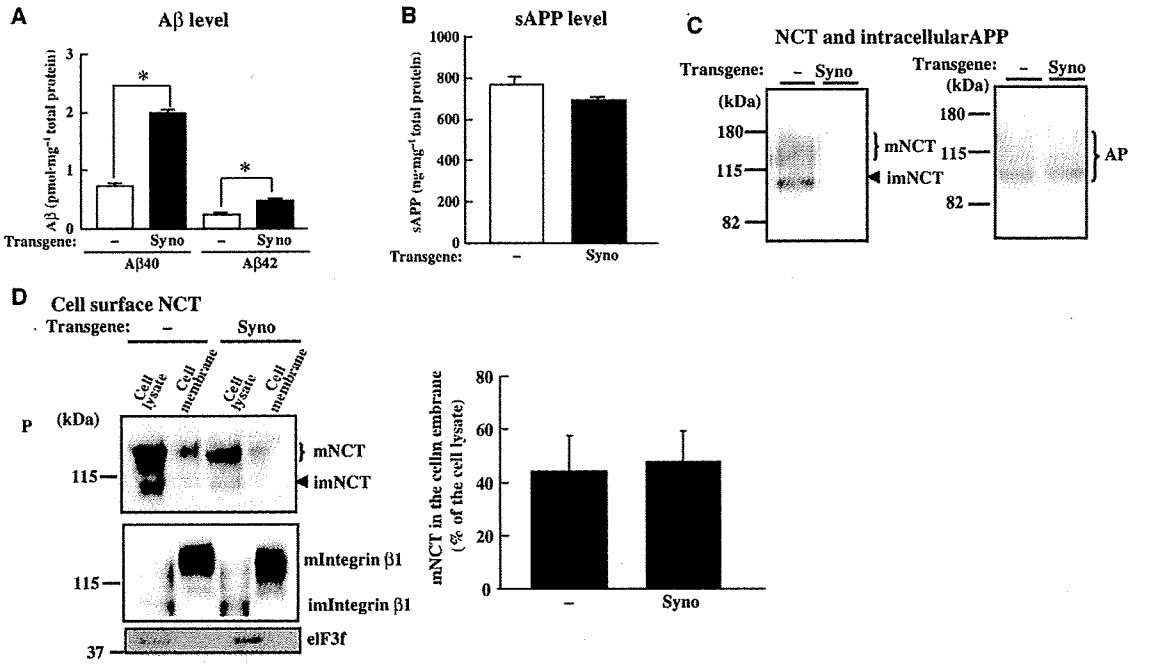

Fig. 5. Effect of the overexpression of Synoviolin on Aβ generation. Wild-type murine fibroblasts expressing APP were retrovirally expressed with Synoviolin. Aβ (A) and soluble APP (B) secreted from the cells during a 96-h culture were detected by ELISA. Values are the means ± SEM of four independent dishes ($n = 4$). Asterisk indicates significant differences from mock [significant difference at $P < 0.01$ (Student's *t*-test)]. (C) NCT and intracellular APP in the cell lysates were immunodetected with anti-NCT IgG and 22C11 respectively. (D) Left panel: cell surface NCT in the mock- or Synovilin-transfected cells was immunodetected as described in Fig. 3. Integrin β1 (as a control for the cell surface protein) and eIF3f (as a control for the cytosolic protein) were also immunodetected. Similar results were obtained from three independent experiments. m integrin β1, mature integrin β1; im integrin β1, immature integrin β1. Right panel: the band intensities were quantified, and the percentage mature NCT level in the cell membrane relative to that of the total cell lysate is shown. Data are the average of three independent experiments. –, mock transfection; Syno, Synoviolin transfection; imNCT, immature NCT; mNCT, mature NCT.

Interestingly, the sugar modification of NCT in *synoviolin*-null cells appeared to be slightly different from that in wt cells. This may suggest that Synovilin-mediated ubiquitination also regulates the trafficking of NCT within the Golgi compartment, because the maturation of the sugar modification of the protein occurs within the Golgi compartment. Recently, there has been an expansion of the recognized roles for ubiquitin in processes other than proteasome-dependent proteolysis, which includes intracellular trafficking (reviewed in [13]). In this regard, it is noteworthy that both immature NCT and mature NCT delivered to the cell surface were increased in *synoviolin*-null cells, although only the mature form of NCT goes to the cell surface in wt cells (Fig. 4). It appears that Synoviolin somehow suppresses the direct delivery of NCT from ER to the cell surface. Previously, it has been shown that Synoviolin increases the membrane localization of huntingtin protein [18], also suggesting that Synoviolin is involved in intracellular trafficking.

We also found that NCT interacts with Synoviolin (Fig. 3), strongly suggesting that NCT is the substrate of Synoviolin. As reported previously, NCT undergoes ubiquitination [24]. We found that the degree of ubiquitination of NCT in wt cells was higher than that in *synoviolin*-null cells. Therefore, NCT is most likely to be a substrate of Synoviolin. However, the other E3 ubiquitin ligase also appears to ubiquitinate NCT, because NCT was ubiqutinated slightly even in *synoviolin*-null cells. Indeed, in *synoviolin*-null cells, NCT started to degrade more than 10 h after cycloheximide treatment (data not shown). Further study of the mechanism underlying NCT degradation mediated by Synoviolin, including an *in vitro* study, is needed.

It was also noted that the overexpression of Synoviolin increased the Aβ level, whereas the cellular level of NCT decreased in transfected cells, because a decreased NCT level would be expected to decrease the Aβ level. Because the levels of full-length APP and soluble APP were not changed (Fig. 5), it is likely that γ-cleavage was increased. As reported previously [25],

the cell membrane NCT level is thought to be more important than the intracellular level of NCT for Aβ generation. Therefore, we investigated whether Synoviolin enhances the cell surface localization of NCT; however, no increase in the cell membrane NCT level in cells transfected with Synoviolin was observed. It has also been shown that the overexpression of SEL-10, that is an E3 ligase for PS1 ubiquitination, causes a decrease in the level of PS1, but an increase in Aβ secretion [26]. This suggests that SEL-10-mediated ubiquitination modulates the PS1 complex in APP processing, although the exact mechanism is not known. Therefore, likewise, Synoviolin-mediated ubiquitination can also regulate Aβ generation, possibly through the modulation of intracellular trafficking. As the overexpression of Synoviolin was suggested to increase γ-cleavage, as mentioned above, the overexpression of Synoviolin, probably through ubiquitination, could promote the trafficking of the PS complex to the site at which γ-cleavage occurs, or activate γ-secretase itself.

In this study, we conclude that Synoviolin is involved in the degradation of immature NCT. We have also shown that the expression of Synoviolin enhances Aβ generation. Further study of the mechanism underlying the enhancement of Aβ generation by Synoviolin will clarify the interaction between the ubiqutination of the PS complex and APP processing.

Materials and methods

Antibodies, reagents and cell lines

A mouse anti-PS1 monoclonal IgG (for the CTF of PS1) was purchased from Chemicon International (Temecula, CA, USA). A rabbit anti-NCT IgG and a mouse NCT monoclonal IgG were purchased from Sigma (St. Louis, MO, USA) and Chemicon International, respectively. MG-132 was purchased from Sigma. A rabbit anti-APH1aL antibody was purchased from COVANCE (Berkeley, CA, USA). Anti-PEN-2 IgM was provided by Dr Thinakaran [27,28]. Anti-α-tubulin and anti-calnexin IgG were purchased from Santa Cruz Biotechnology, Inc. (Santa Cruz, CA, USA). Anti-APP N-terminal antibody 22C11 was purchased from Sigma. Anti-HRD1 (Synoviolin) C-terminal antibody was purchased from ABGENT (San Diego CA, USA). Anti-elF3f was purchased from Rockland Inc. (Gilbertsville, PA, USA). Anti-integrin β1 antibody was purchased from BD Biosciences (San Jose, CA, USA). Monoclonal antibody against mono- and polyubiquitin was purchased from BIOMOL (Plymouth Meeting, PA, USA). Synoviolin-null murine fibroblasts [29] and murine fibroblasts overexpressing human APP were cultured in Dulbecco's modified Eagle's medium (DMEM; Wako Pure Chemical Industries, Ltd., Osaka, Japan) containing 10% fetal bovine serum.

Plasmids and retrovirus-mediated infection

PMX-Synoviolin was generated as described previously [16]. cDNA encoding Synoviolin C307A mutant was generated by overlap PCR using the following primers: 5′-AAATGTGGTTGGCGGGCAGTCTCTTGGC-3′ and 5′-ACTGCCCGCCAACCACATTTTCC-3′. The PCR product was verified by sequencing. The retrovirus-mediated infection was carried out as reported previously [30].

Cycloheximide treatment

Cells (5×10^5) plated on 60 mm tissue culture dishes were grown for 24 h; cycloheximide was then added to a final concentration of 20 $\mu g \cdot mL^{-1}$. At various times after the addition of cycloheximide, the cells were harvested and lysed in RIPA buffer (150 mM NaCl, 10 mM Tris/HCl pH 7.5, 1% Nonidet P-40, 0.1% SDS and 0.2% sodium deoxycholate) containing a protease inhibitor cocktail.

Immunoprecipitation, immunoblotting and ELISA

Cultured cells were lysed in RIPA buffer containing a protease inhibitor cocktail. The solubilized proteins were subjected to immunoprecipitation as described previously [31]. The precipitated proteins were resolved by SDS-PAGE on 4–20% gel for the detection of PS and NCT. Immunoblotting was performed as reported previously [31]. ELISAs for Aβ and soluble APP were performed using a βAmyloid ELISA kit (Wako Pure Chemical Industries, Ltd., Osaka, Japan) and human soluble APP ELISA kit (IBL Co., Ltd., Nagoya, Japan), respectively.

Cell surface biotinylation

Cell surface biotinylation was carried out using a cell surface protein isolation kit (Pierce, Rockford, IL, USA). The cells were grown in four 10 cm tissue culture dishes, and washed twice with ice-cold NaCl/P_i. The cells were incubated in 10 mL of ice-cold sulfosuccinimidy-2-(biotinamido)-ethyl-1,3-dithiopropionate (0.25 $mg \cdot mL^{-1}$) in ice-cold NaCl/P_i for 30 min at 4 °C, and then 500 μL of the quenching solution were added to each dish to quench the reaction. The cells were scraped and washed twice with Tris-buffered saline (TBS) (10 mM Tris/HCl pH 7.5, 150 mM NaCl) and lysed in lysis buffer containing protease inhibitors. Each lysate was incubated with streptavidin–agarose beads at 4 °C for 60 min, and the captured proteins were eluted with 50 mM dithiothreitol in Laemmli's SDS sample buffer.

Acknowledgements

We thank Dr Gopal Thinakaran for providing anti-PEN-2 IgG. This study was supported in part by a grant-in-aid for scientific research from the Ministry of Education, Culture, Sports, Science and Technology of Japan, and by a grant from the Ministry of Health, Labor and Welfare of Japan. We thank Dr Paul Langman for assistance with the English.

References

1 Selkoe DJ (2002) Deciphering the genesis and fate of amyloid β-protein yields novel therapies for Alzheimer disease. *J Clin Invest* **110**, 1375–1381.
2 Vassar R, Bennett BD, Babu-Khan S, Kahn S, Mendiaz EA, Denis P, Teplow DB, Ross S, Amarante P, Loeloff R *et al.* (1999) β-Secretase cleavage of Alzheimer's amyloid precursor protein by the transmembrane aspartic protease BACE. *Science* **286**, 735–741.
3 De Strooper B (2003) Aph-1, Pen-2, and Nicastrin with Presenilin generate an active γ-Secretase complex. *Neuron* **38**, 9–12.
4 Thinakaran G, Borchelt DR, Lee MK, Slunt HH, Spitzer L, Kim G, Ratovitsky T, Davenport F, Nordstedt C, Seeger M *et al.* (1996) Endoproteolysis of presenilin 1 and accumulation of processed derivatives in vivo. *Neuron* **17**, 181–190.
5 Gu Y, Chen F, Sanjo N, Kawarai T, Hasegawa H, Duthie M, Li W, Ruan X, Luthra A, Mount HT *et al.* (2003) APH-1 interacts with mature and immature forms of presenilins and nicastrin and may play a role in maturation of presenilin–nicastrin complexes. *J Biol Chem* **278**, 7374–7380.
6 Kaether C, Lammich S, Edbauer D, Ertl M, Rietdorf J, Capell A, Steiner H & Haass C (2002) Presenilin-1 affects trafficking and processing of βAPP and is targeted in a complex with nicastrin to the plasma membrane. *J Cell Biol* **158**, 551–561.
7 Kim SH, Yin YI, Li YM & Sisodia SS (2004) Evidence that assembly of an active γ-secretase complex occurs in the early compartments of the secretory pathway. *J Biol Chem* **279**, 48615–48619.
8 Yu G, Nishimura M, Arawaka S, Levitan D, Zhang L, Tandon A, Song YQ, Rogaeva E, Chen F, Kawarai T *et al.* (2000) Nicastrin modulates presenilin-mediated notch/glp-1 signal transduction and βAPP processing. *Nature* **407**, 48–54.
9 Leem JY, Vijayan S, Han P, Cai D, Machura M, Lopes KO, Veselits ML, Xu H & Thinakaran G (2002) Presenilin 1 is required for maturation and cell surface accumulation of nicastrin. *J Biol Chem* **277**, 19236–19240.
10 Kimberly WT, LaVoie MJ, Ostaszewski BL, Ye W, Wolfe MS & Selkoe DJ (2002) Complex N-linked glycosylated nicastrin associates with active γ-secretase and undergoes tight cellular regulation. *J Biol Chem* **277**, 35113–35117.
11 Zhang YW, Luo WJ, Wang H, Lin P, Vetrivel KS, Liao F, Li F, Wong PC, Farquhar MG, Thinakaran G *et al.* (2005) Nicastrin is critical for stability and trafficking but not association of other presenilin/γ-secretase components. *J Biol Chem* **280**, 17020–17026.
12 Ratovitski T, Slunt HH, Thinakaran G, Price DL, Sisodia SS & Borchelt DR (1997) Endoproteolytic processing and stabilization of wild-type and mutant presenilin. *J Biol Chem* **272**, 24536–24541.
13 Mukhopadhyay D & Riezman H (2007) Proteasome-independent functions of ubiquitin in endocytosis and signaling. *Science* **315**, 201–205.
14 Pickart CM (2004) Back to the future with ubiquitin. *Cell* **116**, 181–190.
15 Schulze A, Standera S, Buerger E, Kikkert M, van Voorden S, Wiertz E, Koning F, Kloetzel PM & Seeger M (2005) The ubiquitin-domain protein HERP forms a complex with components of the endoplasmic reticulum associated degradation pathway. *J Mol Biol* **354**, 1021–1027.
16 Amano T, Yamasaki S, Yagishita N, Tsuchimochi K, Shin H, Kawahara K, Aratani S, Fujita H, Zhang L, Ikeda R *et al.* (2003) Synoviolin/Hrd1, an E3 ubiquitin ligase, as a novel pathogenic factor for arthropathy. *Genes Dev* **17**, 2436–2449.
17 Christianson JC, Shaler TA, Tyler RE & Kopito RR (2008) OS-9 and GRP94 deliver mutant alpha1-antitrypsin to the Hrd1-SEL1L ubiquitin ligase complex for ERAD. *Nat Cell Biol* **10**, 272–282.
18 Yang H, Zhong X, Ballar P, Luo S, Shen Y, Rubinsztein DC, Monteiro MJ & Fang S (2007) Ubiquitin ligase Hrd1 enhances the degradation and suppresses the toxicity of polyglutamine-expanded huntingtin. *Exp Cell Res* **313**, 538–550.
19 Yamasaki S, Yagishita N, Sasaki T, Nakazawa M, Kato Y, Yamadera T, Bae E, Toriyama S, Ikeda R, Zhang L *et al.* (2007) Cytoplasmic destruction of p53 by the endoplasmic reticulum-resident ubiquitin ligase 'Synoviolin'. *EMBO J* **26**, 113–122.
20 Omura T, Kaneko M, Onoguchi M, Koizumi S, Itami M, Ueyama M, Okuma Y & Nomura Y (2008) Novel functions of ubiquitin ligase HRD1 with transmembrane and proline-rich domains. *J Pharmacol Sci* **106**, 512–519.
21 Gao B, Lee SM, Chen A, Zhang J, Zhang DD, Kannan K, Ortmann RA & Fang D (2008) Synoviolin promotes IRE1 ubiquitination and degradation in synovial fibroblasts from mice with collagen-induced arthritis. *EMBO Rep* **9**, 480–485.
22 Zou K, Hosono T, Nakamura T, Shiraishi H, Maeda T, Komano H, Yanagisawa K & Michikawa M (2008) Novel role of presenilins in maturation and transport of integrin β1. *Biochemistry* **47**, 3370–3378.

23 Sai X, Kokame K, Shiraishi H, Kawamura Y, Miyata T, Yanagisawa K & Komano H (2003) The ubiquitin-like domain of Herp is involved in Herp degradation, but not necessary for its enhancement of amyloid beta-protein generation. *FEBS Lett* **553**, 151–156.
24 He G, Qing H, Tong Y, Cai F, Ishiura S & Song W (2007) Degradation of nicastrin involves both proteasome and lysosome. *J Neurochem* **101**, 982–992.
25 Morais VA, Leight S, Pijak DS, Lee VM & Costa J (2008) Cellular localization of Nicastrin affects amyloid β species production. *FEBS Lett* **582**, 427–433.
26 Li J, Pauley AM, Myers RL, Shuang R, Brashler JR, Yan R, Buhl AE, Ruble C & Gurney ME (2002) SEL-10 interacts with presenilin 1, facilitates its ubiquitination, and alters A-beta peptide production. *J Neurochem* **82**, 1540–1548.
27 Araki W, Takahashi-Sasaki N, Chui DH, Saito S, Takeda K, Shirotani K, Takahashi K, Murayama KS, Kametani F, Shiraishi H *et al.* (2008) A family of membrane proteins associated with presenilin expression and γ-secretase function. *FASEB J* **22**, 819–827.
28 Luo WJ, Wang H, Li H, Kim BS, Shah S, Lee HJ, Thinakaran G, Kim TW, Yu G & Xu H (2003) PEN-2 and APH-1 coordinately regulate proteolytic processing of presenilin 1. *J Biol Chem* **278**, 7850–7854.
29 Yagishita N, Ohneda K, Amano T, Yamasaki S, Sugiura A, Tsuchimochi K, Shin H, Kawahara K, Ohneda O, Ohta T *et al.* (2005) Essential role of synoviolin in embryogenesis. *J Biol Chem* **280**, 7909–7916.
30 Komano H, Shiraishi H, Kawamura Y, Sai X, Suzuki R, Serneels L, Kawaichi M, Kitamura T & Yanagisawa K (2002) A new functional screening system for identification of regulators for the generation of amyloid β-protein. *J Biol Chem* **277**, 39627–39633.
31 Sudoh S, Kawamura Y, Sato S, Wang R, Saido TC, Oyama F, Sakaki Y, Komano H & Yanagisawa K (1998) Presenilin 1 mutations linked to familial Alzheimer's disease increase the intracellular levels of amyloid beta-protein 1–42 and its N-terminally truncated variant(s) which are generated at distinct sites. *J Neurochem* **71**, 1535–1543.
32 Lagirand-Cantaloube J, Offner N, Csibi A, Leibovitch MP, Batonnet-Pichon S, Tintignac LA, Segura CT & Leibovitch SA (2008) The initiation factor eIF3-f is a major target for atrogin1/MAFbx function in skeletal muscle atrophy. *EMBO J* **27**, 1266–1276.

Supporting information

The following supplementary material is available:
Fig. S1. Deglycosylation of NCT.

This supplementary material can be found in the online version of this article.

Please note: As a service to our authors and readers, this journal provides supporting information supplied by the authors. Such materials are peer-reviewed and may be re-organized for online delivery, but are not copy-edited or typeset. Technical support issues arising from supporting information (other than missing files) should be addressed to the authors.

Molecular Neurodegeneration

BioMed Central

Research article

Open Access

Apolipoprotein E4 (1–272) fragment is associated with mitochondrial proteins and affects mitochondrial function in neuronal cells

Toshiyuki Nakamura[1], Atsushi Watanabe[2], Takahiro Fujino[3], Takashi Hosono[1] and Makoto Michikawa*[1]

Address: [1]Department of Alzheimer's Disease Research, National Institute for Longevity Sciences, National Center for Geriatrics and Gerontology, 36-3 Gengo, Morioka, Obu, Aichi 474-8522, Japan, [2]Department of Vascular Dementia, National Institute for Longevity Sciences, National Center for Geriatrics and Gerontology, 36-3 Gengo, Morioka, Obu, Aichi 474-8522, Japan and [3]Department of Bioscience, Integrated Center for Science (INCS), Ehime University, Shizukawa, Shigenobu-cyo, Onsengun, Ehime 791-0295, Japan

Email: Toshiyuki Nakamura - nakamu-t@nifty.com; Atsushi Watanabe - watsushi@nils.go.jp; Takahiro Fujino - tfujino@m.ehime-u.ac.jp; Takashi Hosono - t-hos@nils.go.jp; Makoto Michikawa* - michi@nils.go.jp

* Corresponding author

Published: 20 August 2009

Molecular Neurodegeneration 2009, 4:35 doi:10.1186/1750-1326-4-35

Received: 8 July 2009
Accepted: 20 August 2009

This article is available from: http://www.molecularneurodegeneration.com/content/4/1/35

Abstract

Background: Apolipoprotein E allele ε4 (apoE4) is a strong risk factor for developing Alzheimer's disease (AD). Secreted apoE has a critical function in redistributing lipids among central nervous system cells to maintain normal lipid homeostasis. In addition, previous reports have shown that apoE4 is cleaved by a protease in neurons to generate apoE4(1–272) fragment, which is associated with neurofibrillary tanglelike structures and mitochondria, causing mitochondrial dysfunction. However, it still remains unclear how the apoE fragment associates with mitochondria and induces mitochondrial dysfunction.

Results: To clarify the molecular mechanism, we carried out experiments to identify intracellular apoE-binding molecules and their functions in modulating mitochondria function. Here, we found that apoE4 binds to ubiquinol cytochrome *c* reductase core protein 2 (UQCRC2) and cytochrome C1, both of which are components of mitochondrial respiratory complex III, and cytochrome *c* oxidase subunit 4 isoform 1 (COX IV 1), which is a component of complex IV, in Neuro-2a cells. Interestingly, these proteins associated with apoE4(1–272) more strongly than intact apoE4(1–299). Further analysis showed that in Neuro-2a cells expressing apoE4(1–272), the enzymatic activities of mitochondrial respiratory complexes III and IV were significantly lower than those in Neuro-2a cells expressing apoE4(1–299).

Conclusion: ApoE4(1–272) fragment expressed in Neuro2a cells is associated with mitochondrial proteins, UQCRC2 and cytochrome C1, which are component of respiratory complex III, and with COX IV 1, which is a member of complex IV. Overexpression of apoE4(1–272) fragment impairs activities of complex III and IV. These results suggest that the C-terminal-truncated fragment of apoE4 binds to mitochondrial complexes and affects their activities, and thereby leading to neurodegeneration.

Background

It has been shown that the prevalence of Alzheimer's disease (AD) is associated with the polymorphisms of genes related to cholesterol metabolism, including *apolipoprotein E (apoE)* [1-3], *ATP-binding cassette transporter A1 (ABCA1)* [4], and *CYP46*, the gene encoding cholesterol 24-hydroxylase [5,6]. Human apoE, a 34-kDa protein with 299 amino acids, has three major isoforms, apoE2, apoE3, and apoE4 [7-9]. It is well known that the possession of apoE4 allele is a major risk factor for Alzheimer's disease (AD) [1-3]. The apoE4 allele, which is found in 40–65% of cases of sporadic and familial AD, increases the occurrence and lowers the age of onset of the disease [3,10]. In the central nervous system, apoE is one of the major lipid acceptors [11,12] and interacts with ABCA1 [13] to remove cholesterol from cells and generate high-density lipoprotein (HDL) particles [14] in an apoE-isoform-specific manner [15-18]. Because apoE-HDL is the major cholesterol supplier in the brain and the supply of HDL-cholesterol is essential for synaptogenesis and neurite outgrowth in neurons [19,20], the apoE-isoform-dependent difference in HDL generation may result in the apoE-isoform-dependent difference in the maintenance of synaptic plasticity and the recovery of neurons from neuronal damage found in AD brains.

In addition to the role of apoE in modulating extracellular lipid transport, the isoform-dependent intracellular functions of apoE have also been reported. A previous report has shown that apoE3 recycling is associated with concomitant cholesterol efflux and thereby contributes to the formation of apoE-containing HDL, whereas apoE4 recycling is impaired and apoE4 accumulates within endosomal compartments, inducing an impaired cholesterol efflux [21], which may lead to the accumulation of cellular cholesterol and enhanced amyloid β-protein (Aβ) generation [22]. Another effect of reduced recycling of apoE4 is due to the tight binding of apoE4 to LDLR and LRP1 in the endosomal compartment [21], which in turn affects the interaction of the amyloid precursor protein (APP) and LRP1 that is crucial for the generation of Aβ [23,24]. Other lines of evidence have shown that apoE is cleaved by a protease to generate C-terminal-truncated fragments of apoE (residues 1–272) (apoE4(1–272)) in cultured neuronal cells, and the apoE(1–272) fragment is found in the brains of AD patients and transgenic mice expressing human apoE [25,26]. This proteolytic cleavage occurs in neurons, but not in astrocytes, and C-terminal-truncated fragments of apoE accumulated in an age-dependent manner in the brains of apoE4 mice and, to a significantly lesser extent, apoE3 mice [26]. These fragments, particularly apoE4(1–272), cause AD-like neurodegeneration and memory deficits in transgenic mice expressing apoE4(1–272) [27]. These lines of evidence suggest that the intraneuronal proteolytic processing of apoE could enhance the neuropathology and promote neurodegeneration in AD brains. It has been shown that the presence of a lipid-binding region of apoE (residues 244–272) is critical for apoE fragments to exert neurotoxicity in vivo [27]. Previous studies have shown that residues 267–299 are responsible for the tetramerization of apoE in solution, and the truncation of residues 273–299 in apoE4 gives rise to the monomeric form [28], and that these hydrophobic residues appear to be responsible for the neurotoxicity caused by the C-terminal-truncated apoE4 fragments [29]. In addition to the strong neurotoxicity caused by the apoE4(1–272) fragment, it has been shown that the apoE4(1–272) fragment accumulates in filamentous neurofibrillary tanglelike structures with phosphorylated tau in the cytosol or mitochondria, inducing mitochondrial dysfunction [25-27,29]. However, it still remains unclear how the apoE fragments are transported to the filamentous cytoplasmic structures or to mitochondria, and how they associate with mitochondria and induce mitochondrial dysfunction. To address these questions, we performed experiments to identify the proteins that associate with apoE4(1–272) or intact apoE4(1–299), and determine their functions. We identified three apoE4-binding proteins, all of which are components of mitochondria. We found that these proteins preferentially bind to apoE4(1–272) than to apoE4(1–299) and that the overexpression of apoE4(1–272) fragment decreases the enzymatic activities of mitochondrial respiratory complexes III and IV in cultured cells.

Results

Identification of apoE4-associated proteins

To identify molecules that specifically bind to apoE4, various fractions obtained from mouse brain were loaded onto a FLAG-apoE4(1–272) or FLAG-apoE4(1–299) affinity column. The proteins bound to these columns were eluted with an excess amount of FLAG peptide and the extracts were subjected to SDS-PAGE and silver staining. When each mouse brain fraction was loaded onto a FLAG-apoE4(1–272) or FLAG-apoE4(1–299) affinity column and eluted samples were subjected to SDS-PAGE, many protein bands were detected as candidate apoE4-associated proteins (Fig. 1). These bands were detected only when the mouse brain fractions and FLAG-apoE4 recombinant proteins coexisted.

To identify these proteins, the protein bands were subjected to LC-MS/MS analysis. As a result, we identified sixteen apoE4-associated proteins, which are shown in Table 1. These candidate proteins include the ATP synthase protein α and β subunits, which were previously reported [30]. Interestingly, ten among the candidate proteins are shown to be associated with mitochondria.

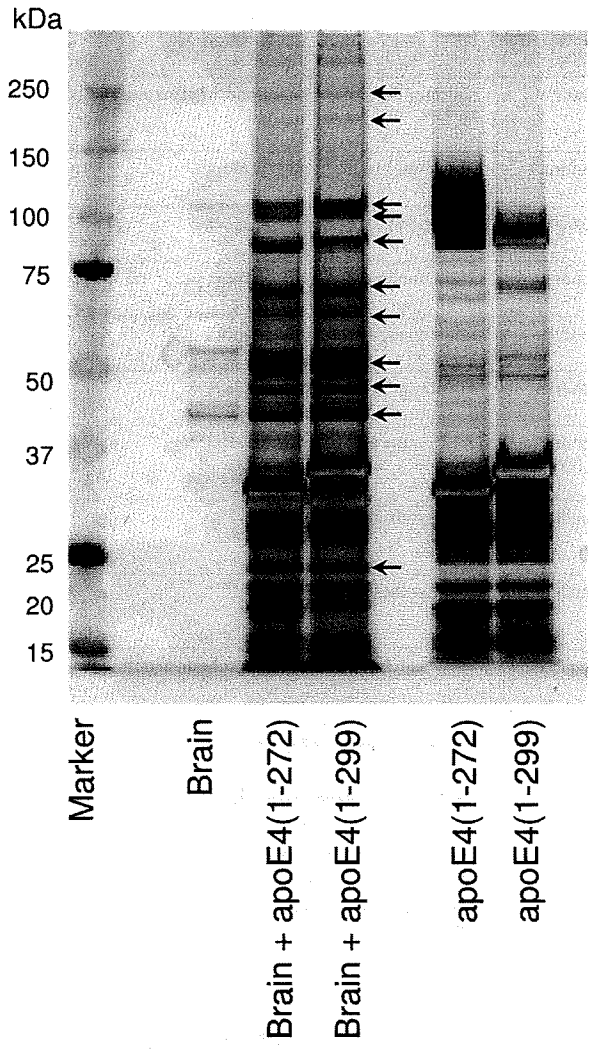

Figure 1
The proteins coimmunoprecipitated with apoE4 in the membrane extracts from mouse brain. Mouse brain membrane extracts were applied to the FLAG-apoE4(1–299) or FLAG-apoE4(1–272)-anti-FLAG M2-agarose affinity resin column and then eluted with the elution buffer. The eluant was dialyzed against the dialysis buffer, concentrated, and subjected to SDS-PAGE. The gels were stained with SilverQuest Silver Staining kit (Invitrogen). The protein bands (arrows), which were absent in the brain samples without apoE4s, and in the apoE4s samples without brain, were subjected to LC-MS/MS analysis.

Association of identified proteins with apoE4 in cultured cells

Next, we examined whether these proteins really associate with apoE in living cells. We cotransfected each candidate protein and FLAG-apoE4 into Neuro2a cells. Twenty-four hours following the transfection, the cells were harvested and treated with Triton X-100 solubilization buffer to obtain cell lysate as described in Materials and Methods. We carried out immunoprecipitation using these samples with an anti-FLAG antibody. The immunoprecipitate was then subjected to western blotting analysis using antibody specific for each protein or anti-HA antibody. This is because, in case we could not find antibodies specific for some candidate proteins, we could still generate HA-tagged proteins. Among the proteins identified by LC-MS/MS analysis, we found that three proteins, ubiquinol cytochrome c reductase core protein 2 (UQCRC2), cytochrome C1, and cytochrome *c* oxidase subunit 4 isoform 1 (COX IV 1) were associated with apoE4(1–299) and apoE4(1–272).

To examine whether mouse UQCRC2 is really associated with apoE proteins in cells, Neuro2a cells were cotransfected with mammalian expression plasmids encoding FLAG-apoE4(1–272) or FLAG-apoE4(1–299) and plasmids encoding mouse UQCRC2. Western blot analysis showed that the signal representing mouse UQCRC2 was clearly detected in the immunoprecipitate from the cells cotransfected with apoE4(1–272), while a very faint signal for UQCRC2 was detected in that from the cells cotransfected with apoE4(1–299). ApoE proteins were similarly immunoprecipitated in both samples (Fig. 2A). These results suggest that UQCRC2 prefers to associate with apoE4(1–272) than with apoE4(1–299).

To examine whether human UQCRC2 also associates with apoE4, we performed an experiment using human HA-tagged UQCRC2 expression vector. Similar to the results using mouse UQCRC2-transfected cells, the signals representing human HA-tagged UQCRC2 were clearly detected in the immunoprecipitate from the cells cotransfected with apoE4(1–272), while a very faint signal for HA-UQCRC2 was detected in that from the cells cotransfected with apoE4(1–299). Under these conditions, apoE4(1–272) and apoE4(1–299) proteins were similarly immunoprecipitated in both samples (Fig. 2B).

Next, we examined the association of human cytochrome C1 and apoE proteins using Neuro2a cells cotransfected with HA-tagged human cytochrome C1 expression vector and plasmids encoding FLAG-apoE4(1–272) or FLAG-apoE4(1–299). A strong signal for HA-tagged human cytochrome C1 was detected in the immunoprecipitate from the cell samples expressing apoE4(1–272), while a very faint signal for cytochrome C1 was detected in those transfected with apoE4(1–299) plasmid. ApoE4(1–272) and apoE4(1–299) proteins were similarly detected in both samples (Fig. 2C).

In addition, whether COX IV 1 is associated with apoE was determined. Human COX IV 1 was immunoprecipitated in the samples from apoE4(1–272)-expressing cells

Table 1: ApoE-associated proteins identified by LC-MS/MS analysis

Protein	Intracellular localization	Function
Solute carrier family 25 (mitochondrial carrier, Aralar) member 12	Mitochondria	Calcium-dependent mitochondrial aspartate and glutamate carrier
Ubiquinol cytochrome c reductase core protein I	Mitochondria	Mitochondrial electron transport
* Ubiquinol cytochrome c reductase core protein 2 (UQCRC2)	Mitochondria	Mitochondrial electron transport
* Cytochrome C1	Mitochondria	Mitochondrial electron transport
Cytochrome oxidase subunit II	Mitochondria	Mitochondrial electron transport
* Cytochrome c oxidase subunit IV isoform 1 (COX IV1)	Mitochondria	Mitochondrial electron transport
ATP synthase, H+ transporting, mitochondrial F1 complex, α subunit, isoform 1	Mitochondria	ATP synthesis
ATP synthase, H+ transporting, mitochondrial F1 complex, β subunit	Mitochondria	ATP synthesis
ATP synthase, H+ transporting, mitochondrial F1 complex, δ subunit	Mitochondria	ATP synthesis
Methylenetetrahydrofolate dehydrogenase (NADP+ dependent)- 1 like	Mitochondria	Folic acid and derivative biosynthetic process
Syntaxin binding protein 1	Cytoplasm	Modulates exocytosis of dense-core granules
Nonmuscle myosin heavy chain	Cytoplasm	Actin filament-based movement
Tubulin, alpha 1A	Cytoplasm	Constituent of microtubules
RAB3A, member RAS oncogene family	Cytoplasm	Involved in exocytosis by regulating a late step in synaptic vesicle fusion.
Progesterone receptor membrane component 1	Plasma membrane	Receptor for progesterone
Cardiotrophin-like cytokine factor 1	Extracellular space	Cell surface receptor linked signal transduction

ApoE4-associated protein bands that were detected with SDS-PAGE were prepared and analyzed as described in the Methods. Asterisks (*) show the apoE-binding proteins identified and characterized in this study.

and a very faint signal for COX IV 1 was detected in the samples from apoE4(1–299)-expressing cells, whereas apoE4(1–272) and apoE4(1–299) proteins were similarly immunoprecipitated in both samples (Fig. 3). Interestingly, these proteins, UQCRC2, cytochrome C1, and COX IV 1, are associated more strongly with apoE4(1–272) than with apoE4(1–299). Concerning other proteins, we carried out similar experiments; however, no association of these proteins with apoE4(1–272) and apoE4(1–299) was found in cultured cells (data not shown).

The levels of apoE4 in mitochondrion-rich fraction isolated from ApoE4(1–272)- or ApoE4(1–299)-expressing cells

The results indicate that apoE4(1–272) binds to mitochondrial proteins; therefore, we next determined whether the levels of apoE4(1–272) and apoE4(1–299) are also associated with the mitochondria. We, thus, determined the levels of apoE4(1–272) and apoE4(1–299) in mitochondrion-rich fractions isolated from Neuro2a cells transfected with apoE4(1–272) or apoE4(1–299). The level of apoE4(1–272) in the pellet, a mitochondrion-rich fraction, was greater than that of apoE4(1–299) (Fig. 4). VDAC, a mitochondrion marker, was recovered in the pellet fraction (Fig. 4).

Effect of apoE4(1–272) overexpression on activities of mitochondrial respiratory complexes

It is known that UQCRC2 and cytochrome C1 are subunits of mitochondrial respiratory complex III and COX IV 1 is a subunit of mitochondrial respiratory complex IV. It

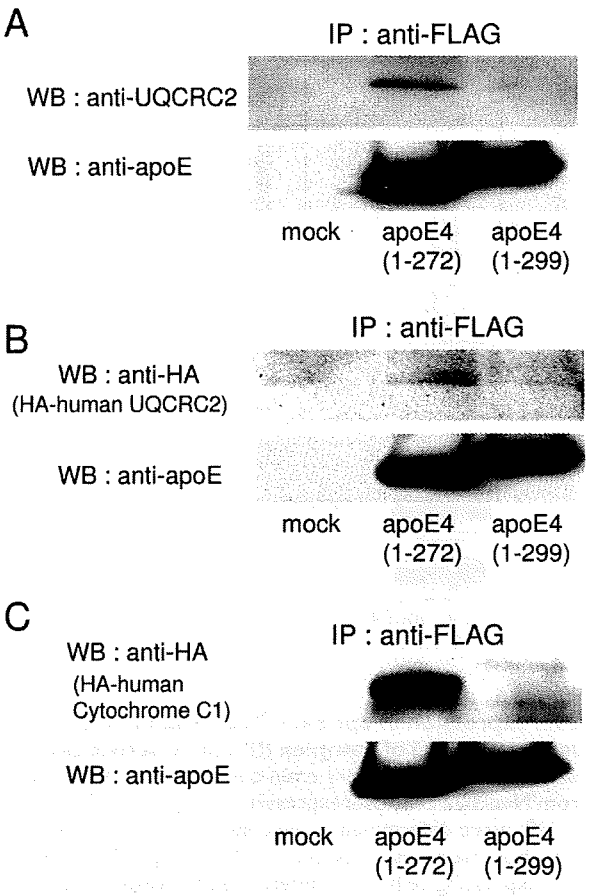

Figure 2
ApoE4 interacts with the subunits of mitochondrial respiratory complex III in Neuro2a cells. Neuro2a cells were cotransfected with mammalian expression plasmids encoding FLAG-apoE4(1–272) or FLAG-apoE4(1–299) and plasmids encoding mouse UQCRC2, human HA-UQCRC2, or human HA-cytochrome C1, all of which are candidate proteins suggested to be associated with apoE4 (Table 1). Twenty-four hours following the transfection, the cells were harvested and treated with 500 μl of Triton X-100 solubilization buffer to obtain cell lysate. The cell lysate was then incubated with anti-FLAG M2-agarose affinity resin, and the protein binding to the affinity column was eluted using FLAG peptide, and the eluted protein was then analyzed by western blotting with anti-UQCRC2 (mouse UQCRC2) antibody (A), anti-HA antibody (human UQCRC2) (B), or anti-HA antibody (human cytochrome C1) (C).

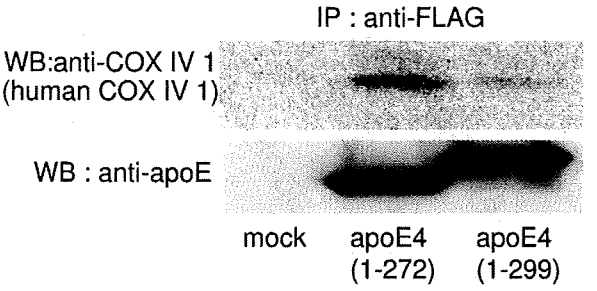

Figure 3
ApoE4 interacts with the subunits of mitochondrial respiratory complex IV in Neuro2a cells. Neuro2a cells were co-transfected with FLAG-apoE4 (1–272 or 1–299) plasmids and mammalian expression plasmids encoding the candidate apoE4-associated proteins. The cells were treated with 500 μl of Triton X-100 solubilization buffer and the cell lysate was incubated with anti-FLAG M2-agarose affinity resin. The immunoprecipitates were then analyzed by western blotting with an anti-COX IV 1 antibody (human COX IV 1).

was reported that apoE4(1–272) induces mitochondrial dysfunction [25-27,29]. Because these proteins are associated more strongly with apoE4(1–272) than with apoE4(1–299), we investigated whether the enzymatic activities of mitochondrial respiratory complexes III and IV change, when apoE4(1–272) is overexpressed in cultured cells. Complex III activity was expressed as the difference in the reduction of cytochrome *c* with or without antimycin A and myxothiazol, both of which are complex III inhibitors. Expectedly, the complex III activity of apoE4(1–272)-overexpressing Neuro2a cells was lower than that of apoE4(1–299)-overexpressing cells (Fig. 5A). Because apoE4(1–272) associates with UQCRC2 and cytochrome C1, there was a possibility that the decrease in complex III activity in Neuro2a cells expressing apoE4(1–272) was due to the interaction between apoE4 and complex III. Complex IV activity was expressed as the difference in the oxidation of ferrocytochrome C with or without KCN and Na_3N, both of which are complex IV inhibitors. The complex IV activity of apoE4(1–272)-overexpressing cells was significantly lower than that of apoE4(1–299)-overexpressing cells (Fig. 5B). The levels of the mitochondrial proteins UQCRC2 and cytochrome C1 in apoE4(1–272)- and apoE4(1–299)-overexpressing cells were similar, as demonstrated by western blot analysis using anti-UQCRC2 and anti-cytochrome C1 antibodies (Fig. 5C).

Effects of overexpression of apoE4(1–272) and apoE4(1–299) on ATP synthase activity and mitochondrial membrane potential

Because apoE4(1–272) decreases the activities of mitochondrial complexes III and IV, we next examined whether the overexpression of apoE4(1–272) also affects ATP synthase activity and mitochondrial membrane potential. Unexpectedly, apoE4(1–272) and apoE4(1–299) showed no effect on ATP synthase activity (Fig. 6A). We further examined the effect of the overexpression of

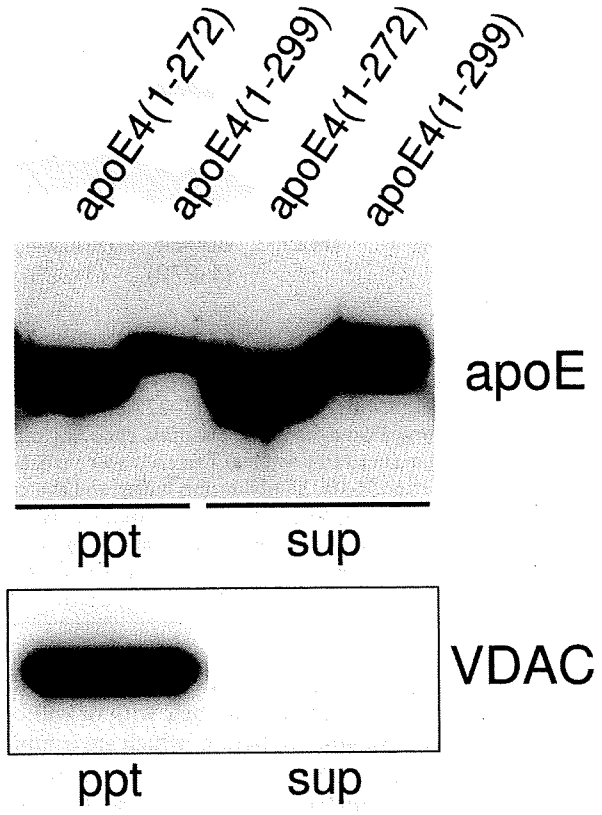

Figure 4
The level of apoE4(1–272) recovered from the mitochondrion-rich fraction is greater than that of apoE4(1–299). Neuro2a cells transfected with ApoE4(1–272) and ApoE4(1–299) plasmids were harvested and homogenized with a homogenizing buffer (10 mM Tris-HCl, pH 7.4, 1 mM EDTA, 0.25 M sucrose), and the resulting homogenate was centrifuged at 1,000 *g* for 10 min at 4°C. The resulting supernatant was further centrifuged at 8,000 *g* for 20 min at 4°C. The resulting precipitate (ppt) was used as the mitochondrion-rich fraction. Equal amounts of proteins from the ppt and supernatant (sup) fractions were analyzed by western blot analysis using the anti-apoE antibody, AB946, and the anti-VDAC antibody. VDAC was used as the mitochondrion marker.

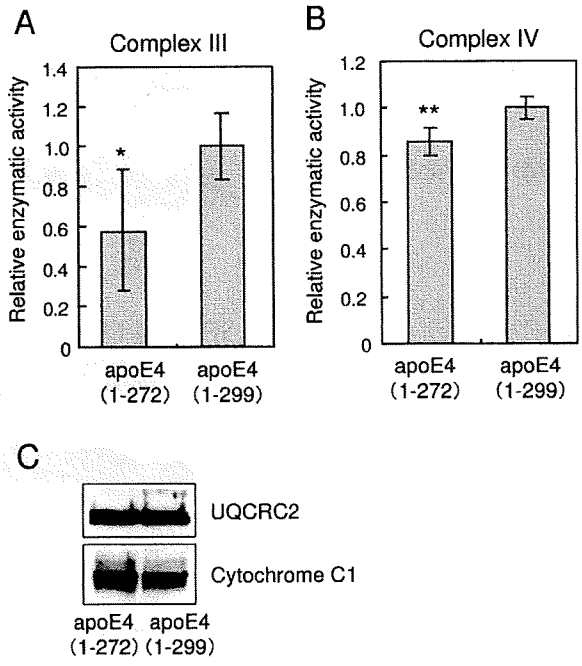

Figure 5
Overexpression of apoE4(1–272) results in the decreased level of complex III and IV activities. Enzymatic assays of respiratory chain complexes III (A) and IV (B) from Neuro2a cells overexpressing FLAG-apoE4(1–272 or 1–299) were determined as described in the Methods. The mitochondria levels in apoE4(1–272)- and apoE4(1–299)-overexpressing cells were determined by western blot analysis using the anti-UQCRC2 and the anti-cytochrome C1 antibodies (C). Data are the mean ± SEM of nine independent experiments. * $P < 0.005$, ** $P < 0.0005$ (t-distribution test).

apoE4(1–272) and apoE4(1–299) on mitochondrial membrane potential. Neuro2a cells transfected with these apoE4 species were stained with JC-1, a fluorescent dye that has been shown to be a reliable indicator of mitochondrial membrane potential changes in intact cells. After three hours of treatment of Neuro2a cells with 1 μM valinomycin, a K^+ ionophore that disrupts the transmembrane electrical gradient, the intensity of red fluorescence (FL2) markedly decreased, whereas that of green fluorescence (FL1) slightly increased, as demonstrated by JC-1 staining (Fig. 6B), indicating the dissipation of mitochondrial membrane potential. On the other hand, there were no significant differences in FL1 and FL2 intensities among Neuro2a cells transfected with mock, apoE4(1–272) and apoE4(1–299) (Figs. 6B, C, and 6D), indicating that the overexpression of apoE4(1–272) and apoE4(1–299) has no effect on mitochondrial membrane potential.

Discussion

Here, we show the molecules associated with apoE protein. Among the molecules identified, we show for the first time that apoE4, particularly C-terminal cleaved apoE4(1–272), binds to UQCRC2 cytochrome C1 and COX IV 1. Although apoE(1–272) has been shown to be translocated to mitochondria, it still remains unclear how the apoE fragments associate with mitochondria and induce mitochondrial dysfunction. The present study has shown that apoE4(1–272) binds to UQCRC2 cytochrome C1, a component of complex III, and COX IV 1, a component of complex IV, and that overexpression of apoE(1–

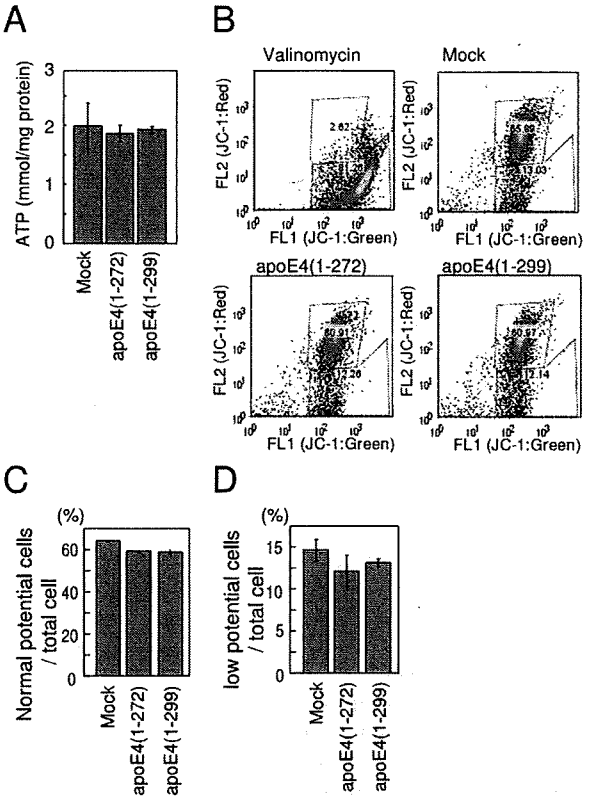

Figure 6
Effects of overexpression of apoE4(1–272) and apoE4(1–299) on ATP synthase activity and mitochondrial membrane potential. The ATP synthase activity in Neuro2a cells transfected with the ApoE4(1–272) and ApoE4(1–299) plasmids were determined (A) as described in the Methods. The data are the mean ± SEM of three experiments. (B) Flow cytometry plots were used to determine the ratio of cells having normal and low mitochondrial membrane potentials, which were demonstrated by staining with the JC-1 dye. The distribution of the cells sorted by FACS was analyzed, and the ratios of the number of cells showing normal membrane potential (C) and low membrane potential (D) to total cell number were calculated.

272) fragment in Neuro2a cells results in decreases in the levels of complex III and complex IV activities compared with those in cells overexpressing intact apoE4. These results suggest that the apoE4(1–272) fragment binds to UQCRC2 cytochrome C1 and COX IV 1, thereby inhibiting complex III and complex IV activities, respectively. The candidate molecules, which may associate with apoE to transport apoE to mitochondria, were not identified in our present analysis (Table 1). This should be addressed in a future study.

Another finding in the present study is that UQCRC2 cytochrome C1 and COX IV 1 are associated more strongly with ApoE4(1–272) than with intact apoE4(1–299) (Figs. 2, 3). There are at least two possible explanations for this result. One explanation is that apoE4(1–272) is structurally different from apoE4(1–299), resulting in the difference in hydrophobicity or binding affinity to other proteins. It has been shown that the C-terminus of apoE (residues 253–289) participates in hydrophobic interactions that stabilize the tetramer [28], and that these hydrophobic residues are suggested to be responsible for inducing neurotoxicity caused by the C-terminal-truncated apoE4 [29]. In addition, a recent study has shown that apoE4 lacking a hydrophobic C-terminal α-helical segment (residues 273–299) found in brain leads to a less organized C-terminal structure that is available for interaction with cell membranes and other proteins such as Aβ [31]. Another explanation is that more apoE(1–272) is translocated to mitochondria than intact apoE(1–299), because the silver staining shows that the intensities of the bands representing apoE-associated proteins were not different between the samples containing apoE4(1–272) and apoE4(1–299) (Fig. 1), whereas the level of apoE4(1–272) was greater than that of apoE4(1–299) in the mitochondrion-rich fraction of Neuro2a cells expressing apoE4(1–272) and apoE4(1–299) (Fig. 4). Although the precise mechanism underlying this difference is yet unknown, it is possible that the truncation of residues 273–299 in apoE4 leads to the reorganization of the C-terminal domain, with a lipid-binding region being less organized and available for hydrophobic interaction including Aβ [31-33].

Regarding the mitochondrial dysfunction in Alzheimer disease, there are previous reports showing that the overexpression of amyloid precursor protein increases the level of Aβ in mitochondria [34], and that mitochondrial complex III and IV activities are decreased in Tg2576 mouse brains [34]. In addition, the complex IV activity was shown to decrease in the brain of AD patients [35-39]. Moreover, it has been shown that the apoE(1–272) fragment is generated at a greater level from apoE4 than apoE3, and the overexpression of apoE isoform-dependently affects mitochondrial function [27]. These lines of evidence together with our present study suggest that the greater level of apoE4(1–272) fragment generated from apoE4 may be associated with Aβ that is transported to mitochondria and binds to UQCRC2 cytochrome C1 and COX IV 1, and causes mitochondrial dysfunction.

Complexes III and IV are related to ATP synthesis and the maintenance of mitochondrial membrane potential, which are critical for cell survival. Thus, we examined the

effect of the transient expressions of apoE4(1–272) and apoE4(1–299) on ATP synthesis and membrane potential in Neuro2a cells. Unexpectedly, there was no difference between apoE4(1–272)- and apoE4(1–299)-transfected cells in terms of the levels of ATP synthesis or membrane potential (Fig. 6). However, when we tried to generate the Neuro2a cells, in which apoE4(1–272) is stably expressed, all the cells were dead within 2 weeks after the transfection, whereas apoE4(1–299)-expressing cells remained alive. These results suggest that apoE4(1–272) may have neurotoxicity as previously reported [29], although the level of toxicity is low. This issue remains to be addressed in further studies.

One may consider that apoE is synthesized as a secretory protein; however, how apoE enters the cytosol remains unclear and controversial. Previous studies have shown that apoE escapes the secretory or endosomal internalization pathway, and enters the cytosol of neuronal cells [25,29,40] and non-neuronal cells [41], whereas another study has failed to show this [42]. Therefore, the physiological relevance of the three mitochondrial proteins that we have identified in this study, which are associated with apoE, remains to be confirmed under physiological conditions.

It is well known that apoE4 is a strong risk factor for AD development, and the regulation of apoE4 function may be a therapeutic target for AD. Our findings indicate that if we could modulate the generation of apoE4(1–272) and/or modulate its translocation to mitochondria, the apoE4-associated induction of neurodegeneration could be prevented or attenuated. Because it has been shown that the C-terminus of the apoE-cleaving enzyme is a neuron-specific, chymotrypsin-like serine protease [25-27], the characterization and modulation of this enzyme activity would be a therapeutic target for AD.

Conclusion

We identified intracellular apoE-binding molecules and determined their functions in modulating mitochondria function. The ApoE-binding molecules we found are ubiquinol cytochrome *c* reductase core protein 2 (UQCRC2), cytochrome C1, and cytochrome *c* oxidase subunit 4 isoform 1 (COX IV 1). The UQCRC2 and cytochrome C1 are components of mitochondrial respiratory complex III, and COX IV 1 is a component of complex IV. Interestingly, these proteins associated with apoE4(1–272) more strongly than intact apoE4 (1–299). When apoE4(1–272) expression level increased in Neuro2a cells, the enzymatic activities of mitochondrial respiratory complexes III and IV were significantly lower than those in Neuro-2a cells expressing apoE4(1–299). These results suggest that the C-terminal-truncated fragment of apoE4(1–272) bind to mitochondrial complexes and affects their activities.

Methods

Preparation of mouse brain membrane extracts and cytosolic fraction

Brains obtained from C57BL6 male mice were homogenized with a homogenizing buffer (10 mM Tris-HCl, pH 7.4 1 mM EDTA 0.25 M sucrose), and the homogenate was centrifuged at 1,000 *g* for 10 min at 4°C. The supernatant was recentrifuged at 10,000 *g* for 20 min at 4°C, and the resulting precipitate was suspended in a homogenizing buffer. The supernatant was recentrifuged at 100,000 *g* for 1 min at 4°C, and the resulting precipitate was suspended in a homogenizing buffer. The supernatant was used as the cytosolic fraction. The proteins in the 10,000 *g* and 100,000 *g* pellet fraction were extracted with homogenizing buffer containing 1 M KCl. The resulting pellet was solubilized with 2% Triton X-100 for 1 h at 4°C and then centrifuged at 100,000 *g* of 1 h at 4°C. The supernatants were used as 10,000 *g* or 100,000 *g* membrane extracts.

FLAG fusion proteins

Recombinant FLAG-apoE4 fusion proteins encoding WT (1–299) or C-terminal truncated apoE4 (1–272) were prepared and purified as follows. PCR products encoding apoE4 (1–272) and apoE4 (1–299) were subcloned into pFLAG-MAC expression vector (Sigma). These plasmids were transformed into the BL21 strain of *Escherichia coli* and induced with isopropyl-1-thio-b-$_D$-galactopyranoside to produce FLAG fusion proteins. The bacteria were suspended in PBS, and vigorous sonication was performed before centrifugation at 10,000 *g* for 20 min. The resulting supernatants were applied to anti-FLAG M2-agarose affinity resin column (Sigma) and then eluted with an elution buffer (TBS containing 100 μg/ml FLAG peptide (Sigma)). Purified FLAG fusion proteins were dialyzed against TBS.

FLAG-ApoE4 affinity chromatography and LC-MS/MS analysis

Recombinant FLAG-apoE4(1–299) or FLAG-apoE4(1–272) fusion protein coupled to anti-FLAG M2-agarose affinity resin was used to identify affinity-purified apoE4-binding proteins. The fractionated mouse brain samples were applied to the FLAG-apoE4(1–299)- and FLAG-apoE4(1–272)-anti-FLAG M2-agarose affinity resin column. The proteins bound to the resin column were then eluted with the elution buffer. The eluted proteins were dialyzed against the dialysis buffer, concentrated, and subjected to SDS-PAGE. The gels were stained with Silver-Quest Silver Staining kit (Invitrogen). The proteins specifically associated with apoEs demonstrated as silver-

stained bands were cut out, digested with trypsin, and subjected to LC-MS/MS analysis.

LC-MS/MS analysis

The proteins in the silver-stained bands were reduced with 10 mM dithiothreitol at room temperature for 2 h and alkylated with 40 mM iodoacetamide in the dark at room temperature for 30 min. Each sample was digested with trypsin (4 μg/ml; Trypsin Gold, Promega) in 40 mM NH_4HCO_3/10%ACN at 37°C overnight. The extracted peptides were then separated via nano liquid chromatography (LC) (Paradigm MS4, Michrom BioResources, Inc., Auburn, CA) using a Magic C18 column (0.2 × 50 mm; Michrom BioResources, Inc.; Auburn, CA). The LC eluent was analyzed using an LCQ Advantage MAX mass spectrometer (Thermo Fisher Scientific) equipped with an ion-spray source. All MS/MS spectra were searched by SEQUEST algorithm from BioWorks software (Thermo Fisher Scientific).

Cells

Neuro2a cells were grown in DMEM medium, supplemented with 10% FBS, 50 units/ml penicillin, 50 mg/ml streptomycin, and 2 mM glutamine at 37°C in a humidified 5% CO_2 95% air incubator.

Transfection of plasmids into cells and co-immunopricipitation

PCR products encoding apoE4 (1–272) and apoE4 (1–299) were subcloned into pFLAG-CMV-2 expression vector (Sigma). Neuro2a cells were co-transfected with FLAG-apoE4 (1–272 or 1–299) plasmids and mammalian expression plasmids coding the candidate of apoE4 associating proteins (Toyobo, Japan) using Lipofectamine 2000 (Invitrogen, CA, USA). As necessary, mammalian expression plasmids coding the candidate apoE4-associated proteins were fused with HA-tag of their C-terminus using KOD-PLUS Mutagenesis Kit (Toyobo). The plasmids were transfected to Neuro2a cells as follows. Neuro2a cells were plated on a 6-cm plate at a cell density of 1.5 × 10^6 and cultured in the culture medium described above. The next day, the ells were transfected with the plasmid employing Lipofectamine 2000 reagent. On culture day 3, the cells were lysed with 500 μl of Triton X-100 solubilization buffer (10 mM Tris-HCl (pH 7.4), 150 mM NaCl, 1 mM EDTA, 10 mg/ml leupeptin, 1 mM PMSF, 0.5% Triton X-100). The cell lysate was incubated with anti-FLAG M2-agarose affinity resin. After an overnight incubation at 4°C, the beads were washed three times with Triton X-100 solubilization buffer and then eluted with the elution buffer (PBS containing FLAG peptide at a concentration of 100 μg/ml). The immunoprecipitates were then analyzed by western blotting with anti-HA monoclonal antibody (Sigma), anti-UQCRC2 monoclonal antibody (Abcam), and anti-COX IV 1 monoclonal antibody (Cell Signaling).

Enzymatic analysis of complexes III and IV

Mitochondria isolated from homogenates of Neuro2a cells transfected with ApoE4 (1–299 or 1–272) were used for enzymatic analysis.

(a) Complex III (Ubiquinol cytochrome c reductase)

The oxidation of $ubiquinol_2$ by complex III was determined using cytochrome *c* (III) as an electron acceptor. The assay was carried out in an assay medium (25 mM potassium phosphate buffer (pH 8.0), 1 mM EDTA, 1 mM KCN, 3 mM Na_3N) supplemented with 20 μM cytochrome *c* (III), and 20 μM $ubiquinol_2$. The reaction was started with 5 μg of mitochondrial protein and the enzyme activity was measured at 550 nm. The activity of complex III is estimated to be the difference in the reduction of cytochrome *c* with and without 10 μg/ml antimycin A and 10 μg/ml myxothiazol.

(b) Complex IV (Cytochrome c Oxidase)

The enzyme activity of cytochrome *c* oxidase (complex IV) was determined using Mitochondria Activity Assay kit (BioChain Institute, U.S.A.) and performed following the manufacture's procedure. Complex IV activity was measured as the oxidation of ferrocytochrome *c* by cytochrome *c* oxidase at 550 nm. Complex IV activity is expressed as the difference in the oxidation of ferrocytochrome C with or without KCN and Na_3N as complex IV inhibitor.

ATP synthase activity assay

Neuro2a cells transfected with apoE4(1–272) and apoE4(1–299) plasmids were harvested and homogenized with a homogenizing buffer (10 mM Tris-HCl, pH 7.4, 1 mM EDTA, 0.25 M sucrose), and the homogenate was centrifuged at 1,000 *g* for 10 min at 4°C. The resulting supernatant was further centrifuged at 10,000 × g for 20 min at 4°C, and the resulting pellet (ppt) fractions were obtained. The ppt fractions were resuspended in 100 μl of assay buffer (1 mM ADP and 5 mM sodium succinate) and incubated for 5 min at 37°C. 100 mM Tris-HCl buffer (pH 7.6) containing 4 mM EDTA was added and the fractions were further incubated for 2 min at 100°C. Then the fractions were plated on ice and ATP level in each fraction was determined using an ATP bioluminescence assay kit CLS II (Roche Diagnosis GmbH, Mannheim, Germany).

Analysis of mitochondrial membrane potential (mt)

ApoE4(1–272 or 1–299)-transfected Neuro2a cells were stained with 2 μM JC-1 (Molecular Probes, Eugene, OR) at 37°C for 20 min. Then, the cells were analyzed using a flow cytometer FACSCalibur (Becton Dickinson, Franklin Lakes, NJ) with FlowJo software (Tree Star Inc., Ashland, OR).

Statistical analysis

StatView computer software (Windows) was used for statistical analysis. Statistical significance of differences

between samples was evaluated by multiple pairwise comparisons among the sets of data using ANOVA and the Bonferoni t-test.

Competing interests

The authors declare that they have no competing interests.

Authors' contributions

TN carried out major part of the experiments. AW carried out TOF-MS/MS analysis and identified molecules associated with apoE. TF generated plasmid containing intact apoE3 and apoE4 cDNA. TH prepared cultured cells. MM designed this study and was involved in the interpretation of the results and in drafting the manuscript.

Acknowledgements

This work was supported by Grant-in-Aid for Scientific Research on Priority Areas-Research on Pathomechanisms of Brain Disorders-from the Ministry of Education, Culture, Sports, Science and Technology of Japan, a grant from the Program for Promotion of Fundamental Studies in Health Sciences of the National Institute of Biomedical Innovation (NIBRO), and a rant from the Ministry of Health, Labor and Welfare of Japan (Comprehensive Research on Aging and Health Grant H20-007).

References

1. Strittmatter WJ, Saunders AM, Schmechel D, Pericak-Vance M, Enghild J, Salvesen GS, Roses AD: **Apolipoprotein E: high-avidity binding to beta-amyloid and increased frequency of type 4 allele in late-onset familial Alzheimer disease.** *Proc Natl Acad Sci USA* 1993, **90:**1977-1981.
2. Roses AD: **Apolipoprotein E affects the rate of Alzheimer disease expression: beta-amyloid burden is a secondary consequence dependent on APOE genotype and duration of disease.** *J Neuropathol Exp Neurol* 1994, **53:**429-37.
3. Corder EH, Saunders AM, Strittmatter WJ, Schmechel DE, Gaskell PC, Small GW, Roses AD, Haines JL, Pericak-Vance MA: **Gene dose of apolipoprotein E type 4 allele and the risk of Alzheimer's disease in late onset families.** *Science* 1993, **261:**921-923.
4. Wollmer MA, Streffer JR, Lutjohann D, Tsolaki M, Iakovidou V, Hegi T, Pasch T, Jung HH, Bergmann K, Nitsch RM, Hock C, Papassotiropoulos A: **ABCA1 modulates CSF cholesterol levels and influences the age at onset of Alzheimer's disease.** *Neurobiol Aging* 2003, **24:**421-426.
5. Kolsch H, Lutjohann D, Ludwig M, Schulte A, Ptok U, Jessen F, von Bergmann K, Rao ML, Maier W, Heun R: **Polymorphism in the cholesterol 24S-hydroxylase gene is associated with Alzheimer's disease.** *Mol Psychiatry* 2002, **7:**899-902.
6. Papassotiropoulos A, Streffer JR, Tsolaki M, Schmid S, Thal D, Nicosia F, Iakovidou V, Maddalena A, Lutjohann D, Ghebremedhin E, Hegi T, Pasch T, Traxler M, Bruhl A, Benussi L, Binetti G, Braak H, Nitsch RM, Hock C: **Increased brain beta-amyloid load, phosphorylated tau, and risk of Alzheimer disease associated with an intronic CYP46 polymorphism.** *Arch Neurol* 2003, **60:**29-35.
7. Mahley RW: **Apolipoprotein E: cholesterol transport protein with expanding role in cell biology.** *Science* 1988, **240:**622-630.
8. Mahley RW, Huang Y: **Apolipoprotein E: from atherosclerosis to Alzheimer's disease and beyond.** *Curr Opin Lipidol* 1999, **10:**207-17.
9. Mahley RW, Rall SC Jr: **Apolipoprotein E: far more than a lipid transport protein.** *Annu Rev Genomics Hum Genet* 2000, **1:**507-37.
10. Farrer LA, Cupples LA, Haines JL, Hyman B, Kukull WA, Mayeux R, Myers RH, Pericak-Vance MA, Risch N, van Duijn CM: **Effects of age, sex, and ethnicity on the association between apolipoprotein E genotype and Alzheimer disease. A meta-analysis. APOE and Alzheimer Disease Meta Analysis Consortium.** *JAMA* 1997, **278:**1349-1356.
11. Roheim PS, Carey M, Forte T, Vega GL: **Apolipoproteins in human cerebrospinal fluid.** *Proc Natl Acad Sci USA* 1979, **76:**4646-4649.
12. Pitas RE, Boyles JK, Lee SH, Hui D, Weisgraber KH: **Lipoproteins and their receptors in the central nervous system. Characterization of the lipoproteins in cerebrospinal fluid and identification of apolipoprotein B, E(LDL) receptors in the brain.** *J Biol Chem* 1987, **262:**14352-14360.
13. Krimbou L, Denis M, Haidar B, Carrier M, Marcil M, Genest J: **Molecular interactions between apolipoprotein E and the ATP-binding cassette transporter A1 (ABCA1): Impact on ApoE lipidation.** *J Lipid Res* 2004, **45:**839-848.
14. Ito J, Zhang LY, Asai M, Yokoyama S: **Differential generation of high-density lipoprotein by endogenous and exogenous apolipoproteins in cultured fetal rat astrocytes.** *J Neurochem* 1999, **72:**2362-2369.
15. Michikawa M, Fan QW, Isobe I, Yanagisawa K: **Apolipoprotein E exhibits isoform-specific promotion of lipid efflux from astrocytes and neurons in culture.** *J Neurochem* 2000, **74:**1008-1016.
16. Gong JS, Kobayashi M, Hayashi H, Zou K, Sawamura N, Fujita SC, Yanagisawa K, Michikawa M: **Apolipoprotein E (ApoE) isoform-dependent lipid release from astrocytes prepared from human ApoE3 and ApoE4 knock-in mice.** *J Biol Chem* 2002, **277:**29919-29926.
17. Xu Q, Brecht WJ, Weisgraber KH, Mahley RW, Huang Y: **Apolipoprotein E4 domain interaction occurs in living neuronal cells as determined by fluorescence resonance energy transfer.** *J Biol Chem* 2004, **24:**25511-25516.
18. Gong JS, Morita SY, Kobayashi M, Handa T, Fujita SC, Yanagisawa K, Michikawa M: **Novel action of apolipoprotein E (ApoE): ApoE isoform specifically inhibits lipid-particle-mediated cholesterol release from neurons.** *Mol Neurodegener* 2007, **2:**9.
19. Mauch DH, Nagler K, Schumacher S, Goritz C, Muller EC, Otto A, Pfrieger FW: **CNS synaptogenesis promoted by glia-derived cholesterol.** *Science* 2001, **294:**1354-7.
20. Hayashi H, Campenot RB, Vance DE, Vance JE: **Glial lipoproteins stimulate axon growth of central nervous system neurons in compartmented cultures.** *J Biol Chem* 2004, **279:**14009-15.
21. Heeren J, Grewal T, Laatsch A, Becker N, Rinninger F, Rye K-A, Beisiegel U: **Impaired Recycling of Apolipoprotein E4 Is Associated with Intracellular Cholesterol Accumulation.** *J Biol Chem* 2004, **279:**55483-55492.
22. Fassbender K, Simons M, Bergmann C, Stroick M, Lutjohann D, Keller P, Runz H, Kuhl S, Bertsch T, von Bergmann K, Hennerici M, Beyreuther K, Hartmann T: **Simvastatin strongly reduces levels of Alzheimer's disease beta-amyloid peptides Abeta 42 and Abeta 40 in vitro and in vivo.** *Proc Natl Acad Sci USA* 2001, **98:**5856-61.
23. Cole SL, Vassar R: **The Alzheimer's disease beta-secretase enzyme, BACE1.** *Mol Neurodegener* 2007, **2:**22.
24. Cam JA, Zerbinatti CV, Li Y, Bu G: **Rapid endocytosis of the low density lipoprotein receptor-related protein modulates cell surface distribution and processing of the beta-amyloid precursor protein.** *J Biol Chem* 2005, **280:**15464-70.
25. Huang Y, Liu XQ, Wyss-Coray T, Brecht WJ, Sanan DA, Mahley RW: **Apolipoprotein E fragments present in Alzheimer's disease brains induce neurofibrillary tangle-like intracellular inclusions in neurons.** *Proc Natl Acad Sci USA* 2001, **98:**8838-43.
26. Brecht WJ, Harris FM, Chang S, Tesseur I, Yu GQ, Xu Q, Dee Fish J, Wyss-Coray T, Buttini M, Mucke L, Mahley RW, Huang Y: **Neuron-specific apolipoprotein e4 proteolysis is associated with increased tau phosphorylation in brains of transgenic mice.** *J Neurosci* 2004, **24:**2527-34.
27. Harris FM, Brecht WJ, Xu Q, Tesseur I, Kekonius L, Wyss-Coray T, Fish JD, Masliah E, Hopkins PC, Scearce-Levie K, Weisgraber KH, Mucke L, Mahley RW, Huang Y: **Carboxyl-terminal-truncated apolipoprotein E4 causes Alzheimer's disease-like neurodegeneration and behavioral deficits in transgenic mice.** *Proc Natl Acad Sci USA* 2003, **100:**10966-71.
28. Fan D, Li Q, Korando L, Jerome WG, Wang J: **A monomeric human apolipoprotein E carboxyl-terminal domain.** *Biochemistry* 2004, **43:**5055-64.
29. Chang S, Ma Tr, Miranda RD, Balestra ME, Mahley RW, Huang Y: **Lipid- and receptor-binding regions of apolipoprotein E4**

fragments act in concert to cause mitochondrial dysfunction and neurotoxicity. *Proceedings of the National Academy of Sciences* 2005, **102:**18694-18699.
30. Mahley RW, Hui DY, Innerarity TL, Beisiegel U: **Chylomicron remnant metabolism. Role of hepatic lipoprotein receptors in mediating uptake.** *Arteriosclerosis* 1989, **9:**114-8.
31. Tanaka M, Vedhachalam C, Sakamoto T, Dhanasekaran P, Phillips MC, Lund-Katz S, Saito H: **Effect of carboxyl-terminal truncation on structure and lipid interaction of human apolipoprotein E4.** *Biochemistry* 2006, **45:**4240-7.
32. Pillot T, Goethals M, Najib J, Labeur C, Lins L, Chambaz J, Brasseur R, Vandekerckhove J, Rosseneu M: **Beta-amyloid peptide interacts specifically with the carboxy-terminal domain of human apolipoprotein E: relevance to Alzheimer's disease.** *J Neurochem* 1999, **72:**230-7.
33. Phu MJ, Hawbecker SK, Narayanaswami V: **Fluorescence resonance energy transfer analysis of apolipoprotein E C-terminal domain and amyloid beta peptide (1–42) interaction.** *J Neurosci Res* 2005, **80:**877-86.
34. Caspersen C, Wang N, Yao J, Sosunov A, Chen X, Lustbader JW, Xu HW, Stern D, McKhann G, Yan SD: **Mitochondrial Abeta: a potential focal point for neuronal metabolic dysfunction in Alzheimer's disease.** *Faseb J* 2005, **19:**2040-1.
35. Takahashi RH, Milner TA, Li F, Nam EE, Edgar MA, Yamaguchi H, Beal MF, Xu H, Greengard P, Gouras GK: **Intraneuronal Alzheimer abeta42 accumulates in multivesicular bodies and is associated with synaptic pathology.** *Am J Pathol* 2002, **161:**1869-79.
36. Martin BL, Schrader-Fischer G, Busciglio J, Duke M, Paganetti P, Yankner BA: **Intracellular Accumulation of beta-Amyloid in Cells Expressing the Swedish Mutant Amyloid Precursor Protein.** *J Biol Chem* 1995, **270:**26727-26730.
37. Chui DH, Tanahashi H, Ozawa K, Ikeda S, Checler F, Ueda O, Suzuki H, Araki W, Inoue H, Shirotani K, Takahashi K, Gallyas F, Tabira T: **Transgenic mice with Alzheimer presenilin 1 mutations show accelerated neurodegeneration without amyloid plaque formation.** *Nat Med* 1999, **5:**560-4.
38. Wilson CA, Doms RW, Lee VM: **Intracellular APP processing and A beta production in Alzheimer disease.** *J Neuropathol Exp Neurol* 1999, **58:**787-94.
39. Hartmann T: **Intracellular biology of Alzheimer's disease amyloid beta peptide.** *Eur Arch Psychiatry Clin Neurosci* 1999, **249:**291-8.
40. Lovestone S, Anderton BH, Hartley C, Jensen TG, Jorgensen AL: **The intracellular fate of apolipoprotein E is tau dependent and apoe allele-specific.** *Neuroreport* 1996, **7:**1005-8.
41. Hamilton RL, Wong JS, Guo LS, Krisans S, Havel RJ: **Apolipoprotein E localization in rat hepatocytes by immunogold labeling of cryothin sections.** *J Lipid Res* 1990, **31:**1589-603.
42. DeMattos RB, Thorngate FE, Williams DL: **A test of the cytosolic apolipoprotein E hypothesis fails to detect the escape of apolipoprotein E from the endocytic pathway into the cytosol and shows that direct expression of apolipoprotein E in the cytosol is cytotoxic.** *J Neurosci* 1999, **19:**2464-73.